EFFECT OF Li, Na, K AND Cs ON VACUUM DECOMPOSITION OF TETRAAMMINEPLATINUM(II) IN ZEOLITES. CATALYTIC ACTIVITY IN CO + NO REACTION*

Jana NOVAKOVA**, Libor BRABEC and Ludmila KUBELKOVA

J. Heyrovsky Institute of Physical Chemistry,
Academy of Sciences of the Czech Republic, 182 23 Prague 8, The Czech Republic

Received October 27, 1994
Accepted December 5, 1994

$[Pt(NH_3)_4]^{2+}$ ions were exchanged for alkali (Li, Na, K and Cs) in -X and -Y zeolites and decomposed in vacuum. TPR after this decomposition showed that autoreduction accompanying this process reduced roughly 2/3 of all Pt^{2+} to Pt^0. The extent of the autoreduction rose with the ammonia pressure over the zeolite. The decomposition rate increased with increasing electropositivity of the alkali ion and this effect completely overlapped that of the zeolite structure. The CO + NO reaction rate also increased from Li to Cs, but -X zeolites were substantially more active than the -Y ones. Oxygen layer on the resulting Pt catalyst affected positively the reaction rate. The dispersion of Pt particles was relatively low, when compared to that obtained by decomposition of the Pt tetraammine complex in oxygen followed by hydrogen reduction. However, the reaction rate was higher.

Very high Pt dispersion and stability of Pt clusters created in zeolites has been achieved by decomposing $Pt(NH_3)_4$ ions exchanged in alkali (predominantly Na) zeolites. The way of the decomposition (decomposition medium, temperature, heating rate) has been reported to affect substantially the Pt particle size and location[1–8]. The highest dispersion was obtained by slow calcination followed by reduction which method gave Pt^0 clusters predominantly in zeolite supercages. The decomposition in vacuum accompanied by autoreduction was found to yield Pt^0 clusters of 1 and 4 nm in diameter, located within the zeolite structure. The direct reduction led to the formation of large Pt^0 clusters on the zeolite exterior.

As one aim of our studies is to look for the most convenient Pt state in zeolites for the CO + NO reaction, we have examined different modes of the decomposition of tetraammineplatinum(II) complexes. Present contribution concerns: (i) the decomposition in vacuum (the path and the extent of autoreduction) and (ii) the reactivity of thus

---

* Presented at the *XXVIth Czech and Slovak Symposium on Catalysis, Prague, November 7 – 8, 1994.*

**The author to whom correspondence should be addressed.

prepared samples in NO + CO reaction. In both cases, the effect of various alkali ions is investigated as well as that of the zeolite type (faujasites X and Y).

Preparation of Pt Clusters by Vacuum Decomposition of Tetraammineplatinum(II) Ions in Zeolites

The following assumptions on the decomposition of $Pt(NH_3)_4^{2+}$ in vacuum have been reported:

Minachev[9] found formation of a Pt surface hydride (positively charged) in Y zeolite at 350 °C:

$$Pt(NH_3)_4^{2+} \rightarrow PtH^+ + H^+ + \text{gaseous products} \tag{A}$$

This hydride exhibited a characteristic IR band at 2 120 cm^{-1}, and underwent the subsequent reduction to Pt^0 at 500 °C.

Jaeger, Schulz-Ekloff et al. found the release of nitrogen during the vacuum decomposition of Pt tetraammine complexes[10–13]. They assume the following decomposition path:

$$[Pt(NH_3)_4]^{2+} \rightarrow [Pt(NH_3)_x]^{2+} + (4 - x)\ NH_3 \ . \tag{B}$$

this occurs below 200 °C, and, above this temperature, the autoreduction of Pt^{2+} can take place in two reactions:

$$\begin{gathered} [Pt(NH_3)_x]^{2+} \rightarrow Pt^0\text{–}(NH) + 2\ H^+ + (x - 1)\ NH_3 \\ 2\ Pt^0\text{–}(NH) \rightarrow 2\ Pt^0 + N_2 + H_2 \ . \end{gathered} \tag{C}$$

If the H_2/N_2 ratio equals 1 and NH_3/N_2 ratio equals 6, the complete Pt autoreduction proceeds. This was found with lower Pt loading, i.e. below 4 $Pt(NH_3)_4^{2+}$ per supercage.

Winkler et al.[14] suggested the following subsequent reactions (using proton spin relaxation technique together with mass spectrometric detection of nitrogen released):

$$[Pt(NH_3)_4]^{2+} \rightarrow Pt^{2+} + 4\ NH_3 \tag{D}$$

$$3\ Pt^{2+} + 2\ NH_3 \rightarrow 3\ Pt^o + 6\ H^+ + N_2 \ . \tag{E}$$

CO + NO Reaction

Platinum is one of the metals which are able to reduce NO to N_2 by oxidation of CO to CO_2, and has been extensively studied from the viewpoint of the removal of NO and CO from car exhaust gases[15].

A lot of papers deal with this reaction and with its individual steps on clean Pt surfaces and on individual crystal planes using UHV methods and instruments (e.g. ref.[16]). Simultaneously, alumina and silica supported Pt also are studied[17]. Less attention has been devoted to the CO + NO reaction over Pt in zeolites, in which the high Pt dispersion can be of great importance.

The most simple individual steps in the CO + NO reaction on Pt are assumed to be as follows[18]:

$$\mathrm{NO} \rightarrow \mathrm{NO_{ads}} \rightarrow \mathrm{N_{ads}} + \mathrm{O_{ads}} \tag{F}$$

$$\mathrm{CO} + \mathrm{O_{ads}} \rightarrow \mathrm{CO_{2\,ads}} \rightarrow \mathrm{CO_2} \tag{G}$$

$$2\,\mathrm{N_{ads}} \rightarrow \mathrm{N_2}\ , \tag{H}$$

where the recombination of N atoms or the dissociation of NO can be the rate determining steps. The recombination was assumed to proceed more rapidly on less dispersed Pt[18–21]. However, formation of N_2O during NO reduction by CO was also reported and its function as a by-side product and/or direct intermediate has been discussed[22]. Including N_2O into the reaction steps, further reactions can be considered.

$$2\,\mathrm{NO} \rightarrow \mathrm{N_2O_{ads}} + \mathrm{O_{ads}} \tag{I}$$

$$\mathrm{N_{ads}} + \mathrm{NO_{ads}} \rightarrow \mathrm{N_2} + \mathrm{O_{ads}} \tag{J}$$

EXPERIMENTAL

Catalysts. $Pt(NH_3)_4Cl_2$ (Aldrich Chemicals) was ion exchanged into alkaline-X and -Y zeolites at room temperature. The parent zeolites NaX (Si/Al = 1.25) and NaY (Si/Al = 2.5) were supplied by Serva International, Germany, and by VURUP, The Slovak Republic, respectively. These Na forms also were, prior to the introduction of tetraammine complexes, ion exchanged for Li, K and Cs. The chemical composition of the samples (obtained by AAS) prior to dehydration and decomposition of ammine ligands is listed in Table I.

Decomposition of tetraammineplatinum(II) in vacuum. The parent hydrated zeolite (2 – 3 mg) was evacuated for 2 h at 100 °C (no difference if the evacuation was carried out overnight) and then decomposed with the heating rate 10 °C min^{-1} directly into the vacuum system of a QMG 420 Balzers quadrupole mass spectrometer; an auxiliary vacuum system was also connected so that the maximum pressure near the decomposing sample did not exceed 10^{-1} Pa. The mass spectra were continuously saved during the decomposition. N_2 and CO cannot be distinguished in the ion 28; a part of this ion can certainly be related to CO, as simultaneously CO_2 was released. Another set of vacuum decomposition was carried out with higher weight of the parent samples (20 mg), which weight was employed in catalytic measurements. The effect of the sample weight (2 – 60 mg) on the composition of gas products was also examined (i.e. effect of the pressure during the decomposition which reached maximum value of 2 Pa for the highest sample weight). For TPR measurements, the decomposition in an oxygen stream was also carried out (with a heating rate of 2 °C min^{-1}) up to 400 °C using 100 mg of the parent sample.

TPR measurements. The undried sample (100 mg) was decomposed in vacuum in a small U reactor whose endings were sealed off after the decomposition, and broken in the TPR apparatus at low temperature (–78 °C). Hydrogen (3 vol.%) in argon (600 ml h^{-1}) were led through this reactor and the TPR was measured within (–18) – 25 °C and 25 – 400 °C. The hydrogen consumption was measured using thermal conductivity cells. Rapid cooling of the sample after the end of the reduction allowed to determine the amount of hydrogen sorbed on the reduced sample (this value was confirmed by measuring the desorption using a flash to 400 °C; cooling and flashing can be several times repeated).

The TPR measurements were also performed with the samples slowly calcinated to 400 °C (2 °C min^{-1}), at which temperature they were held for 4 h. The reduced samples, both those originally treated in vacuum as well those prepared via calcination, were reoxidized in an oxygen stream at 400 °C for 2 h and the TPR was repeated.

TABLE I
Pt content and ion exchange (in %) of zeolites employed

Sample	Pt, wt.%[a]	Ion exchange	
		Pt	alkali
Pt-LiX	3.22 (3.0)	7	Li: 57
Pt-LiY	2.53 (2.4)	9	Li: 44
Pt-NaX	2.46 (2.5)	6	
Pt-NaY	2.49 (2.4)	9	
Pt-KX	2.56 (2.8)	7	K: 84
Pt-KY	2.47 (2.3)	9	K: 92
Pt-CsX	1.83 (2.1)	5	Cs: 39
Pt-CsY	2.61 (3.0)	11	Cs: 52

[a] Per g of wet sample, Pt per unit cell is in brackets.

CO + NO reaction was studied under static conditions (CO : NO mixtures 1 : 1, pressure of 200 Pa, volume 400 cm^3, heating rate 10 °C min^{-1}) on samples (18 mg) thermally decomposed in vacuum in a temperature programmed conversion mode (TPC). The temperatures of the 50% conversion of NO were compared over the individual samples, which were employed just after the vacuun decomposition. The same TPC was performed over samples which were either after or before the first catalytic run allowed to react with 200 Pa of O_2 or NO at 400 °C. After short evacuation and cooling of the sample, the TPC was repeated. These samples are denoted by the index ox; the above oxidation concerned of about 1/5 – 1/10 of all the Pt atoms present.

The progress of the CO + NO reaction was checked leaking a small amount of the gas phase into a Balzers QMG 421 quadrupole mass spectrometer. In some cases, the time-dependence of the reaction was also registered under isothermal conditions.

The gases employed were supplied by Linde (CO, O_2, Ar + H_2, H_2), Messer Griesheim (NO), Aldrich (^{13}CO, 98 at.%), purity >99.99%.

RESULTS

Gas Phase Analysis During Thermal Decomposition of Pt Tetraammine in Alkali Exchanged -X and -Y Zeolites

Products evolved into the gas phase during decomposition of 18 mg of the $Pt(NH_3)_4$ alkali-X and -Y zeolites are shown in Fig. 1, and the individual temperatures of the peaks are listed in Table II. It can be seen, that ammonia is released in two peaks, the low-temperature (LT) one being roughly 3 times higher than the high-temperature (HT) peak. For comparison, the deammoniation of the NH_4^+-X and -Y forms are also included (Fig. 1, dotted curves). The positions of both the LT and HT peaks are shifted to lower temperature with the increasing atomic number of the alkali ion. One exception is exhibited by Cs, for which the decrease of the temperature of the LT peak is less pronounced while the temperature of the HT peak is even higher. The temperatures of both

TABLE II
Temperature (°C) of LT and HT ammonia peaks during decomposition of 18 mg of $Pt(NH_3)_4$-alkali-X and -Y zeolites and NH_4X and -Y zeolites

Alkali	–X Zeolite		–Y Zeolite	
	LT	HT	LT	HT
Li	285	400	280	390
Na	260	340	265	340
K	230	300	230	320
Cs	210	390	230	350
NH_4	170	–	210	–

LT and HT ammonia peaks are roughly the same on -X and -Y zeolites with the same alkali ion. They are higher in all cases than those of the NH_4 zeolites (for which the temperature of the less acid -X zeolite is lower than for Y of higher acidity strength). In agreement with ref.[10], the LT peak is accompanied by the appearance of the $m/z = 28$ ion, which can be related to N_2 (due to autoreduction), but at least partially also to CO (as simultaneously CO_2 is evolved in majority of the measurements, which is shown in Fig. 2).

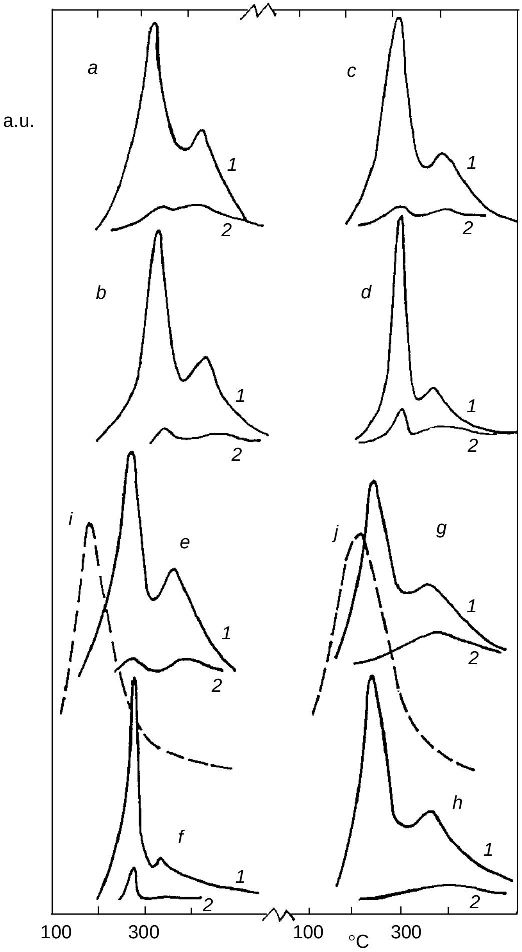

FIG. 1

Ammonia (*1*) and N_2 (+ CO) (*2*) (diminished by factor 4) evolved during the vacuum decomposition of Pt tetraammine ligands in alkali-X and -Y zeolites (18 mg of the wet sample). *a*, *b* Pt-LiX and -Y; *c*, *d* Pt-NaX and -Y; *e*, *f* Pt-KX and -Y; *g*, *h* Pt-CsX and -Y; dotted lines: *i* NH_4-X, *j* NH_4-Y

The evolution of the ion 28 (N_2 + CO), CO_2 and H_2 was studied in more detail with low sample weight (2 mg), when the gases released could be led directly into the mass spectrometer without any leak. In these cases, the evolution of the ion 28 during the LT peak of ammonia was relatively very low; higher intensity of the ions 28, 44 and 2 was observed at temperatures higher than that of the HT peak of ammonia (Fig. 2*a*; the same behaviour was exhibited by all alkali exchanged $Pt(NH_3)_4^{2+}$ zeolites). For that reason, the evolution of the gases was checked on $Pt(NH_3)_4$-NaX zeolite in dependence on the zeolite weight, with lower weight without any leak, above the weight of 10 mg using a needle valve. The maximum pressure of the gases evolved for the highest sample weight in the vicinity of the sample was 2 Pa. The results of these experiments

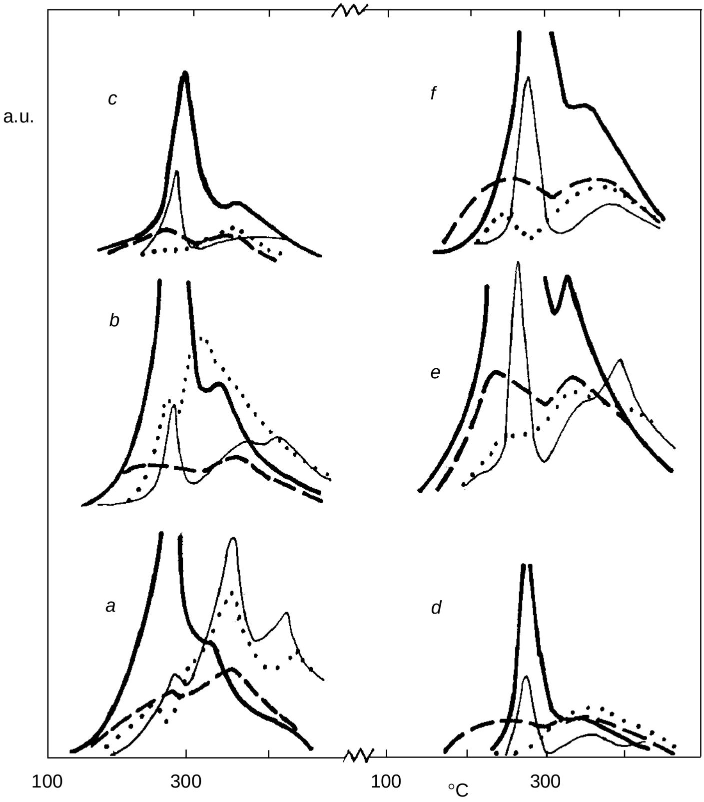

FIG. 2
Effect of the sample weight on the composition of gases released during vacuum decomposition of Pt tetraammine complex in NaX zeolite. *a* 2.8 mg, *b* 6.8 mg, *c* 17.4 mg, *d* 20 mg, *e* 41 mg, *f* 43 mg; two first samples measured using direct connection to the mass spectrometer, the remaining samples connected via a needle-valve; thick full line: ammonia, thin full line: N_2 + CO, dashed line: CO_2, dotted line: H_2 (the curve for H_2 is enlarged by factor 1.7)

are given in Fig. 2*a* – 2*d*, from which it follows that the fraction of the ion 28 (in Fig. 2 cf. the heights of the ion 28 with the HT ammonia peak) is the higher, the higher is the sample weight. However, simultaneously increases the fraction of ion 44 (CO_2), so that again a part of the ion 28 most probably originates from the evolved CO (CO and CO_2 from surface carbonates). The amount of hydrogen released is lower in the LT ammonia peak than that of N_2 (and CO). Even at higher temperatures, the fraction of hydrogen is sometimes lower than that of the ion 28 (in Fig. 2, ions 28, 44 and 2 are displayed as CO + N_2, CO_2 and H_2, using the relevant calibration).

Temperature Programmed Reduction (TPR)

TPR curves are shown in Fig. 3 for $Pt(NH_3)_4$-NaX decomposed in vacuum (Fig. 3*a*) and compared with the same zeolite after decomposition in an oxygen stream (Fig. 3*b*). Full curves stand for the sample after the decomposition, dashed curves for TPR after reoxidation (in an oxygen stream at 400 °C for 2 h) following the first TPR run. The TPR curves within (–18) – (+25) °C were obtained after the cooling bath was removed and the sample allowed to reach room temperature. Peaks on the right-hand side correspond to the consumption of hydrogen during rapid cooling of the sample after TPR to room temperature (the same area of hydrogen evolved can be obtained during the flash

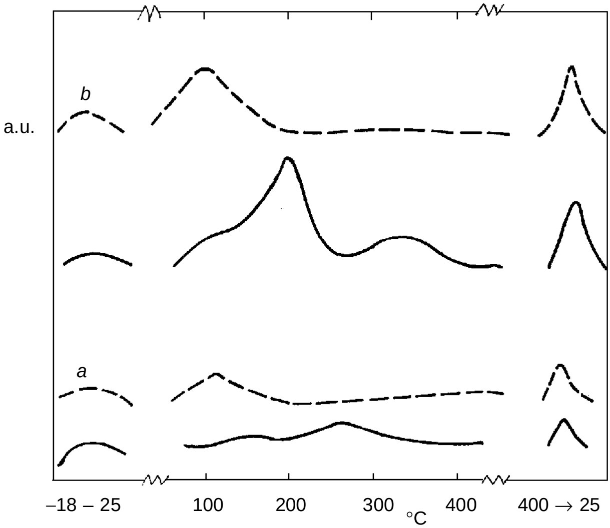

FIG. 3
TPR curves of Pt-NaX prepared via vacuum decomposition (*a*) and via calcination (*b*). Full lines: after the above decompositions, dashed lines: after reoxidation following the first TPR

to 400 °C, which processes (cooling and flashing accompanied by hydrogen adsorption and desorption, respectively) can be repeated.

It can be seen that after reoxidation the TPR peaks are shifted to lower temperature and the adsorption slightly increases. However, the vacuum-decomposed samples cannot be oxidized to the Pt state obtained by decomposition via calcination in an oxygen stream, which follows from Fig. 3 (cf. dashed curve *a* that in the case of full Pt oxidation should be the same as the dashed curve *b*). In Table III, the amounts of hydrogen consumed in TPR after the decomposition in vacuum are listed, together with the H/Pt ratio calculated from the adsorption of hydrogen during rapid cooling after the TPR. It follows that the amounts of hydrogen needed for the reduction are of about three times lower than would correspond to the reduction of PtO or Pt^{2+}.

CO + NO Reaction

The temperature programmed conversion over samples prepared by decomposition in vacuum, both just after the decomposition as well as after the partial oxidation at 400 °C with 200 Pa of O_2 (before or after the first catalytic run) are compared in Table IV (the temperature of 50% conversion of NO is shown). It can be seen that the rate of CO + NO conversion increases from Li to K (for Pt-CsY being almost the same as for Pt-KY; the relatively low Cs content in Pt-CsX most probably decreases the reaction rate), and is substantially higher on -X than on -Y zeolites. H-forms without Pt exhibit very low activity. The (partial) oxidation at 400 °C, concerning only 1/5 – 1/10 of the total number of Pt atoms, increases the reaction rate, for -Y zeolites over all samples, for -X zeolites over Li and Cs samples. However, if the reaction was studied isothermally at 220 °C, the positive effect of the partial oxidation was observed even with Pt-NaX and

TABLE III
Hydrogen consumed (H_2, μmol g^{-1}) during the TPR of tetraammineplatinum(II) ions in alkali-X and -Y zeolites after decomposition in vacuum and H/Pt ratios $(H/Pt)_{exp}$ calculated from hydrogen adsorbed after TPR

Sample	H_2[a]	H_{2exp}[b]	$(H/Pt)_{exp}$
Pt-LiX	170	58	0.34
Pt-LiY	128	54	0.42
Pt-NaX	126	60	0.48
Pt-NaY	128	34	0.27
Pt-KX	131	45	0.34
Pt-KY	127	45	0.35

[a] Theoretical value for Pt(II); [b] experimental value.

Pt-KX. This is shown in Fig. 4 for the isothermal CO + NO reaction over Pt-NaX just after the decomposition in vacuum (Fig. 4*a*), and after the partial oxidation (Fig. 4*b*). In Figs 4*c* and 4*d* (for the sample after vacuum decomposition and partial oxidation, respectively), the isothermal CO + NO reaction over Pt-NaY is also shown, using ^{13}CO: the labelling was employed to distinguish N_2O from CO_2 in the ion $m/z = 44$, and N_2 from CO in the ion $m/z = 28$. It can be seen, that the fraction of N_2O (ion 44) is very low. In both cases (4*a*, 4*b* and 4*c*, 4*d*), the favourable effect of the sample oxidation can be clearly seen.

TABLE IV
Temperature of 50% conversion of NO in NO + CO reaction

Sample	°C[a]	Sample	°C[a]
HNaX	380	HNaY	>400
Pt-LiX	270 (224)	Pt-LiY	320 (284)
Pt-NaX	212 (212)	Pt-NaY	311 (260)
Pt-KX	180 (180)	Pt-KY	294 (245)
Pt-CsX	245 (202)	Pt-CsY	300 (250)

[a] Values in brackets stand for the samples after partial oxidation at 400 °C.

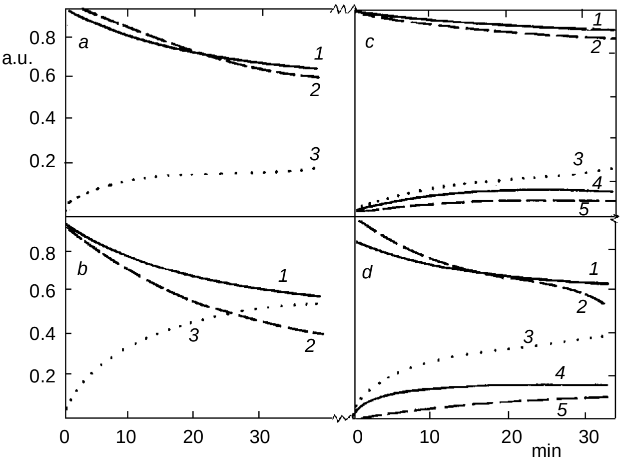

FIG. 4
CO + NO reaction at 220 °C on the samples decomposed in vacuum (*a*), (*c*) and on the partially oxidized samples (*b*), (*d*). *a*, *b* Pt-NaX, 800 Pa, *1* CO + N_2, *2* NO (+ N_2O), *3* CO_2 (+ N_2O); *c*, *d* Pt-NaY, 200 Pa, *1* ^{13}CO, *2* NO, *3* CO_2, *4* N_2, *5* N_2O

The typical TPC (temperature programmed conversion) course is given in Fig. 5: the 50% loss of NO (ion 30) was employed to compare the individual reaction rates over alkali exchanged Pt zeolites. It can be seen that the ion 28 after the initial decrease (consumption in CO + NO reaction) begins to increase due to the formation of N_2. The contribution of N_2O to the ions 44 (molecular peak of N_2O with 100% abundance) and 30 (30% fragment of the molecular ion $m/z = 44$) was neglected in Table IV, as their contributions were very small, which was confirmed using ^{13}CO.

DISCUSSION

Decomposition of the Pt Tetraammine Complex in Vacuum

According to refs[3,10–13] Pt should be completely reduced after the decomposition of $Pt(NH_3)_4$-zeolite due to the autoreduction. This conclusion was based on the analysis of the gases released during the decomposition. In the present measurements it appeared that the fraction of N_2 and H_2 released increases with the increasing sample weight (increasing pressure of the released ammonia), and the N_2/H_2 ratio is higher than 1. The autoreduction unambiguously occurs, but its extent derived from the analysis of the gas phase should be taken with caution; especially, it is necessary to determine, whether the ion 28 can be related to nitrogen only. In our measurements, ion 28 was found to be usually accompanied with ion 44, which agrees with the assumption on the decomposition of surface carbonates. The ratio of the ion 28 to the amount of ammonia released does not seem to be, therefore, the only proof of the complete autoreduction. It is tempting to consider the observation of the increasing fraction of nitrogen (but not hydrogen) with the increased weight of the sample (increased pressure of evolved ammonia) as a result of the secondary reduction of Pt with ammonia according to Eqs[14] (*D*) and (*E*). The uncomplete autoreduction of Pt during the decomposition in vacuum

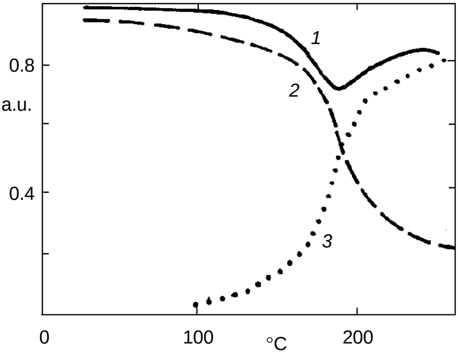

FIG. 5
CO + NO TPC over Pt-NaX after vacuum decomposition. *1* CO + N_2, *2* NO (+ N_2O), *3* CO_2 (+ N_2O)

stems from the TPR measurements: these were carried out with the maximum sample weight of 100 mg, employed in our experiments, i.e. with the highest pressure of ammonia released. Even in this case, reduction roughly corresponding to 1/3 of the total Pt amount was found (Table III).

As concerns the effect of different alkali ions, it can be concluded, that their presence enhances the decomposition rate of the tetraammine complexes; the almost same temperatures of the peak maxima on -X and -Y zeolites with the same alkali ion point to the predominating influence of the alkali ion over that of the zeolite matrix. The decomposition rate increases with the increasing electropositivity of the alkali ion (from Li to Cs), i.e. with the increasing basicity of the zeolite oxygens, and with the increasing alkali weight and size.

Dispersion of Pt after the Decomposition of Pt Tetraammine in Zeolites under Vacuum Heating

Schulz-Ekloff et al.[3,12] reported on the bimodal Pt dispersion after the decomposition of the ammine ligands in less ion-exchanged X zeolites: particles with the average diameters of 1 and 4 nm were found using TEM. Gallezot[2] described the formation of 0.6 – 1.3 nm Pt particles (8 – 14 Pt atoms, all accessible for hydrogen) fitting into Y zeolite supercages (after calcination and reduction at 300 °C) on which the ratio of adsorbed hydrogen, H/Pt, was equal to 1. Chmelka et al.[5] showed (^{129}Xe NMR, hydrogen chemisorption, TEM), that after the to-date most convenient pretreatment conditions, calcination and reduction at 400 °C, the fraction of Pt in supercages is 0.74 and H/Pt ratio equals 1. Our values of the H/Pt ratio, obtained with the samples after calcination followed by reduction, were within 0.6 – 0.9. However, after the decomposition in vacuum and subsequent TPR, this ratio was found to be substantially lower (of about 0.2 – 0.3). Such low values can be explained by the location of hardly reducible Pt in sodalite cages[2], or by the formation of large Pt clusters. The location of all Pt atoms in inaccessible positions does not seem to be probable, as the samples prepared by the vacuum decomposition are at least as active (usually even more active) in CO + NO reaction as the samples prepared by calcination and reduction. Considering the literature data[2,3,6,7,11,12], formation of large particles during the decomposition in vacuum seems to be the most probable reason of the low H/Pt ratio. This is supported by the finding, that the oxidation of the samples (originally prepared in vacuum) after the TPR does not occur quantitatively (see Fig. 3, TPR after reoxidation). According to ref.[7], formation of a thin oxide layer on the Pt cluster preventing the complete oxidation can be assumed. Therefore, formation of relatively large Pt clusters after the vacuum decomposition of Pt tetraammine ligands seems to be more probable than their location in inaccessible positions. However, these clusters have to be located within the zeolite pores, as XPS measurements have not shown any enrichment of the surface layers by Pt (ref.[24]).

CO + NO Reaction

It is evident from Table IV, that the CO + NO reaction proceeds at substantially higher rate over alkali-exchanged PtX than over -Y zeolites; the rate also increases from Li to Cs (with the exception of Pt-CsY, which behaves similarly to Pt-KY). This is in contrast to the decomposition of the tetraammine ligands, which rate was the same for -X and -Y zeolites and was influenced by the nature of the alkali ion only. The positive effect of alkali ions, namely of potassium, on the activation of CO over Pt was found[23]; such effects most probably also operate in the CO + NO reaction, where especially the NO activation can be affected. The dissociation of CO has not been frequently considered in the reaction scheme, however, it was described by Bischoff et al.[12], and also observed in our experiments[24]. The extent of this CO dissociation does not seem to be high and its effect on the reaction mechanism has not yet been elucidated. The influence of the zeolite structure is, opposite to the $Pt(NH_3)_4$ decomposition, evident: the reaction proceeds with substantial higher rate over -X than over -Y zeolites.

More rapid reaction over all Pt zeolites after treatment of the zeolites in an oxidizing atmosphere (O_2 or NO, formation of an oxidized Pt layer) can be most probably related to the initiation via CO reaction with adsorbed oxygen, forming vacancies necessary for the dissociation of NO, which again completes the oxygen surface layer. The conversion of NO to N_2O and N_2 was observed on reduced samples[24].

As concerns the effect of the particle size on the rate of CO + NO reaction, the samples prepared in vacuum with small H/Pt ratio (large clusters), seem to be at least of the same activity as those prepared via calcination and subsequent reduction (higher H/Pt ratios). The positive effect of large Pt clusters on the recombination of N atoms and/or dissociation of NO, reported in refs[17–21], might be the reason of this behaviour.

Formation of N_2O was also found in a small extent during the CO + NO reaction. This was proved using ^{13}CO, that enabled to distinguish CO_2 and N_2O in the ion $m/z = 44$, and N_2 and CO in the ion $m/z = 28$. Special experiments carried out with N_2O + CO reaction showed that this occurs at substantially higher temperatures than the CO + NO reaction. One can, therefore, assume that the reaction via N_2O is only a by-side reaction; however, Cho[22] has found that the sticking coefficient of N_2O on Rh is extremely small, which negatively influences the rate of the CO + N_2O reaction. If N_2O_{ads} is formed as an intermediate of CO + NO reaction, it reacts very quickly with CO, so it almost does not appear as a final product in the CO + NO reaction. If this also occurs over Pt catalyst, the low reaction rate of N_2O + CO needs not to be an unambiguous proof against the reaction route via N_2O.

The results can be summarized as follows:

1. The increasing electropositivity and size of the alkali ion increase the decomposition rate of the Pt tetraammine ligands and the action of the alkali ion exceeds that of the zeolite structure (X or Y zeolite).

2. The CO + NO reaction proceeds with higher rate over -X than over -Y zeolite and is, in both cases, positively affected by the presence of alkali ions in order Li < Na < K ≥ Cs.

3. The decomposition of the $Pt(NH_3)_4$ ligands in vacuum leads to the uncomplete autoreduction of Pt, and to lesser dispersion of Pt particles.

4. The CO + NO reaction proceeds more rapidly, or at least with the same velocity, on larger Pt clusters than on the small ones.

5. Oxidized surface layers on Pt catalysts accelerate substantially the CO + NO reaction.

This study was supported by the grants of the Grant Agency of the Academy of Sciences of the Czech Republic No. 440105 and the Grant Agency of the Czech Republic No. 202/93/0245.

REFERENCES

1. Dalla Betta R. A., Boudart M.: *Proceedings of the 5th International Congress on Catalysis, Palm Beach 1972*, Vol. 2, p. 1329. North Holland, Amsterdam 1973.
2. Gallezot P.: Catal. Rev. Sci. Eng. *20*, 122 (1979).
3. Exner D., Jaeger N., Kleine A., Schulz-Ekloff G.: J. Chem. Soc., Faraday Trans. *84*, 4097 (1988).
4. Tzou M. S., Teo B. K., Sachtler W. M. H.: J. Catal. *113*, 220 (1988).
5. Chmelka B. F., de Menorval L. C., Csencsits R., Ryoo R., Liu S. B., Radke C. J., Petersen E. E., Pines A. in: *Structure and Reactivity of Surfaces* (C. Morterra, A. Zecchina and G. Costa, Eds), p. 269. Elsevier, Amsterdam 1989.
6. Chmelka B. F., Rosin R. R., Went G. T., Bell A. T., Radke C. J., Peterson E. E. in: *Zeolites: Facts, Figures, Future* (P. A. Jacobs and R. A. van Santen, Eds), p. 995. Elsevier, Amsterdam 1989.
7. Chmelka B. F., Went G. T., Csencsits R., Bell A. T., Petersen E. E., Radke C. J.: J. Catal. *144*, 506 (1993).
8. Sachtler W. M. H., Zhang Z.: Adv. Catal. *39*, 129 (1993).
9. Mashchenko A. I., Bronnikov Q. D., Dmitriev R. V., Garinin V. I., Kazansky V. B., Minachev Kh. M.: Kinet. Katal. *15*, 1603 (1974).
10. Exner D., Jaeger N. I., Moeller K., Schulz-Ekloff G.: J. Chem. Soc., Faraday Trans. 1 *78*, 3537 (1982).
11. Jaeger N. I., Jourdan A., Schulz-Ekloff G., Kleine A., Ryder P. L. in: *Studies in Surface Science and Catalysis* (P. J. Grobet, W. J. Mortier, E. F. Vansant and G. Schulz-Ekloff, Eds), Vol. 37, p. 191. Elsevier, Amsterdam 1988.
12. Bischoff H., Jaeger N. I., Schulz-Ekloff G.: Z. Phys. Chem. (Leipzig) *271*, 1093 (1990).
13. Schulz-Ekloff G., Jaeger N. I.: Catal. Today *3*, 459 (1988).
14. Winkler H., Ebert A., Ebert W., Riedel E.: Surf. Sci. *50*, 565 (1975).
15. Taylor K. C.: Catal. Rev. Sci. Eng. *35*, 457 (1993).
16. Hopkinson A., King D. A.: Chem. Phys. *177*, 433 (1993).
17. Altman E. J., Gorte R. J.: J. Catal. *110*, 191 (1988).
18. Fink T., Krischer K., Imbihl R.: J. Vac. Sci. Technol., A *10*, 2440 (1992).
19. Altman E. J., Gorte R. J.: J. Phys. Chem. *93*, 1993 (1989).
20. Veser G., Imbihl R.: J. Chem. Phys. *96*, 7155 (1992).

21. Kaspar J., de Leitenburg C., Fornasiero P., Trovarelli A., Graziani M.: J. Catal. *146*, 136 (1994).
22. Cho B. K.: J. Catal. *148*, 697 (1994).
23. Garfunkel E. L., Crowel J. E., Somorjai G. A.: J. Phys. Chem. *86*, 310 (1982).
24. Novakova J.: Unpublished results.